Recycling Space Debris as a Stepping Stone Towards a Permanent Lunar Presence

Heumassej, Y.; Cervone, A.; Vincent-Bonnieu, S.

DOI
10.52202/078374-0015

Publication date
2024

Document Version
Final published version

Published in
22nd IAA Symposium on Building Blocks for Future Space Exploration and Development - Held at the 75th International Astronautical Congress, IAC 2024

Citation (APA)
Heumassej, Y., Cervone, A., & Vincent-Bonnieu, S. (2024). Recycling Space Debris as a Stepping Stone Towards a Permanent Lunar Presence. In *22nd IAA Symposium on Building Blocks for Future Space Exploration and Development - Held at the 75th International Astronautical Congress, IAC 2024* (pp. 134-144). (Proceedings of the International Astronautical Congress, IAC). International Astronautical Federation, IAF. https://doi.org/10.52202/078374-0015

IAC-24- D3.2A.11x85890

Recycling Space Debris as a Stepping Stone Towards a Permanent Lunar Presence

Y. Heumassej[a,c]*, A. Cervone[b], S. Vincent-Bonnieu[c]

[a] *Department of Space Systems Engineering, Delft University of Technology, Kluyverweg 1, 2629 HS Delft, The Netherlands,* yannickheumassej@ziggo.nl
[b] *Department of Astrodynamics & Space Missions, Delft University of Technology, Kluyverweg 1, 2629 HS Delft, The Netherlands*
[c] *European Space Agency, Directorate Human and Robotic Exploration, Keplerlaan 1, NL-2200 AG Noordwijk-ZH, The Netherlands*
* Corresponding Author

Abstract
This study proposes the concept of recycling space debris as a novel means of supplying material resources for the establishment of a permanent Lunar presence while simultaneously cleaning up Earth's orbital environment. Upon the creation of a space debris dataset and characterizing debris objects as resources and reserves, spent Ariane 5 upper stages in GTO are identified as prime candidates for recycling. However, orbital transfer alignment poses a critical challenge due to orbit perturbations over time. Mission scenarios, including debris capture, transfer and Lunar processing, are analyzed, with global mission energy expenditure used to compare them to direct material delivery missions. Both chemical and electric propulsion transfer architectures are highlighted as enabling feasible and efficient recycling mission scenarios, with potential energy savings of up to 30% per kg of material. The significant reduction in launch mass as a direct consequence of capturing the mission payload in orbit allows for the inclusion of rideshare configurations, increasing efficiency to over 60% less energy investment per kg.
Keywords: Space debris, Moon, Lunar exploration, recycling, in-orbit servicing, low-thrust propulsion

Nomenclature

C_p	Specific heat coefficient
E	Energy
H	Enthalpy
Q	Heat
i	Inclination
J_2	J_2 coefficient
L	Latent heat
M	Mass
n	Mean motion
p	Semi-latus rectum
R_E	Radius of Earth
T	Temperature
V	Velocity
Δ	Change
Ω	Right Ascension of the Ascending Node
ω	Argument of periapsis

Acronyms/Abbreviations

API	Application Programming Interface
AoP	Argument of Periapsis
DISCOS	Database and Information System Characterising Objects in Space
ESC-A	Etage Supérieur Cryotechnique de type A
ESA	European Space Agency
GTO	Geostationary Transfer Orbit
GEO	Geosynchronous Earth Orbit
ISRU	In-Situ Resource Utilization
IADC	Inter-Agency Space Debris Coordination Committee
LEO	Low-Earth Orbit
LLPM	Lower Liquid Propulsion Module
LTO	Lunar Transfer Orbit
MON	Mixed Oxides of Nitrogen
MMH	Monomethyl Hydrazine
MMT	MiniMegaTORTORA
NIST	National Institute of Standards of Technology
NTO	Nitrogen Tetroxide
NORAD	North American Aerospace Defense Command
RAAN	Right Ascension of the Ascending Node
TLE	Two-Line Element
ULPM	Upper Liquid Propulsion Module

1. Introduction

For the first time since the end of the Apollo programme in 1972, mankind has set its sights back onto the Moon. This time with the intent to stay. Spearheaded by the Artemis programme, the establishment of a permanent human presence on the Moon is a crucial milestone for the advancement of human space exploration. The space industry has grown exponentially in recent history, with launch traffic increasing by over 130% since 2020, and over 4300% since 2010 [1]. However, in our efforts to both explore and commercialize the space environment, it has gotten polluted. Old rocket stages and inactive satellites now litter the space around Earth. Where it was once an afterthought, space debris has become one of the space industry's most critical problems. Despite continued efforts to reduce the impact of space debris and safeguard Earth's orbital environment, long-term debris mitigation strategies remain an essential need for the future. But while the majority of currently established efforts focus strictly on the removal of debris, space debris could potentially be leveraged as a source of raw material resources. The Argonaut, the European Space Agency's (ESA) Lunar lander, is envisioned to be Europe's autonomous access to the Lunar surface in the near future. With a 2100 kg payload mass [2] and a 115 €M launch cost of Ariane 64 [3], establishing a Lunar base would cost billions in launch costs alone. Raw material resources recycled from space debris could be an invaluable supplement for the establishment and continued growth of a permanent Lunar presence. While a Lunar base would ideally rely on In-Situ Resource Utilization (ISRU), proposed ISRU efforts for the extraction of metals are often highly complex. Additionally, key alloying metals like zinc and copper are scarce in the Lunar regolith (53 and 18 ppm, respectively) [4], thus limiting the manufacturing of high-performance alloys. The recycling of space debris could be a more readily achievable stepping stone for the establishment of a Lunar base while simultaneously clearing debris from Earth's orbit.

This paper presents a fundamental baseline of understanding for a space debris recycling mission for Lunar applications by designing and optimizing various energy-efficient mission scenarios. Written in collaboration with the European Space Agency this paper addresses the concept of a space debris recycling mission from the viewpoint of complete European autonomy.

2. Methodology & Mission Architecture

The recycling of space debris is a novel and relatively unexplored concept, especially within the context of Lunar exploration activities. In order to investigate the merit of such a mission concept, this paper presents an exploratory study which focuses on both mission feasibility as well as viability. Feasibility represents whether a mission can be performed at all, while viability represents whether the mission is sustainable. Regarding a concept as novel as recycling space debris, strong evidence for feasibility as well as viability is required for such a mission concept to be considered for further study.

This work focuses primarily on single-target space debris return missions as a baseline. That is, a single mission targets a single space debris object for recycling. The overall mission architecture is presented in Figure 1. Various mission scenarios were analyzed in order to capture a broad potential solution space within this defined mission architecture.

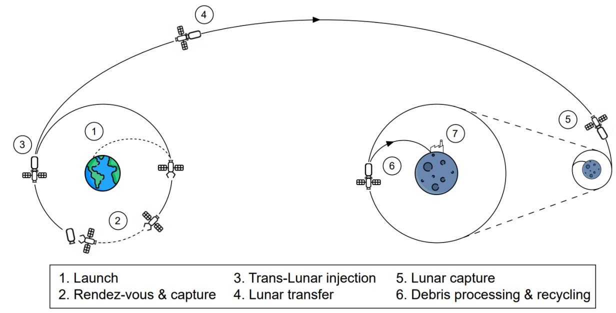

Figure 1. Space debris recycling mission architecture.

Rather than relying on economic cost estimations, it was chosen to compare mission scenarios based on total energy expenditure as the defining metric for mission viability assessment. Here, energy expenditure represents the total energy spent throughout the entire process of turning space debris into raw materials. Whereas economic cost is complex to quantify for novel missions and is subject to significant uncertainty over longer periods of time, the energy "cost" is a more objective and readily accessible metric. Considering the exploratory nature of this study, energy cost is particularly powerful as a comparative metric to assess the merit of various mission scenarios that, though being substantially different, are similar in their core architecture. A space debris recycling mission can in many ways be seen from the perspective of a manufacturing process rather than a traditional space mission. The mission, here, is the transportation and recycling of space debris into raw materials. Energy, particularly embodied energy, is a metric often used for the study and comparison of such manufacturing processes [5]. Additionally, the use of energy, or exergy, has been demonstrated for the analysis of advanced space mission concepts [6]. As such, it was chosen to adopt this approach to assess the recycling of space debris from a global mission perspective.

The Lunar surface was identified as the ideal location for a recycling infrastructure, avoiding the complexities of establishing and operating an orbital recycling station. The presence of gravity and the wealth of space available on the Lunar surface allow for the adaptation of well understood Earth-based recycling practices. Additionally, proposed space debris recycling missions typically leave debris behind in orbit, as not every piece of a space debris object can be recycled. By moving the recycling operations to the Lunar surface, true net zero operation can be achieved. Given the complexity of even a preliminary design for the Lunar segment, defining the design, build-up and operation was considered beyond the scope of this study. It was therefore assumed that the required recycling infrastructure was already present on the Lunar surface. As a result of this assumption, the energy analysis represents only the energy cycle of the complete recycling process and not the establishment of the required infrastructure.

Finally, in order to facilitate a meaningful assessment of the merit of a space debris recycling mission, an adequate reference case must be established as an alternative to be compared against. For this study, the direct delivery of raw materials to the Moon using a Lunar lander mission was considered for direct comparison. In particular, the use of ESA's Argonaut lander was studied, which remains consistent with the viewpoint of European autonomy established for this study.

3. Space Debris Identification & Analysis

In order to establish a baseline understanding of the space debris population currently in orbit around Earth, a comprehensive space debris dataset was generated and analyzed. Based in this analysis, an optimal space debris target was selected.

3.1 Generating a Space Debris Dataset

The Database and Information System Characterising Objects in Space (DISCOS), as published by ESA's Space Debris Office [7], was used as the basis for the space debris dataset, using the Application Programming Interface (API). Other databases such as the Celestrak [8] database were used as supplementary resources to create a comprehensive dataset of all debris in orbit. Through the analysis of this dataset, a total debris mass of 6887.4 metric tons was found to orbit Earth as of the data acquisition date (June 2023). Rocket bodies make up the majority of this debris with a mass fraction of 58.1%, with inactive satellite platforms making up a combined 39.5%. The remaining 2.4% consists of a wide assortment of objects typically low in mass, including payload adapters, radiator covers, de-spin weights etc.

Two-Line Element (TLE) sets published by the United States Space Command [9] were used to extract orbital tracking data. Using this data, orbital analysis of the entire dataset could be performed. A simulation of the orbits of all space debris objects is shown in Figure 3.

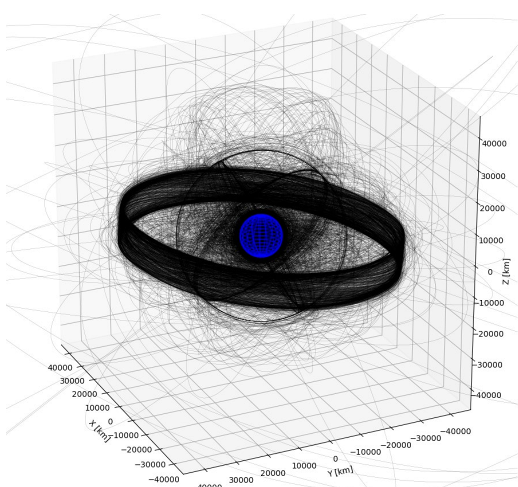

Figure 2. Visualization of debris orbits for all actively tracked space debris objects.

Two main regions of high density can be observed, specifically around Low-Earth Orbit (LEO) and in a band near Geostationary Orbit (GEO). This band is inclined at approximately 15° as a result of Luni-Solar interactions [10]. In order to get an overview of the spatial mass distribution of debris, Figure 3 presents a mapping of the space debris cumulative mass distribution as a function of the semi-major axis up to a value of 50000 km. Debris in higher orbits does exist, but represents such little mass that it is comparatively negligible.

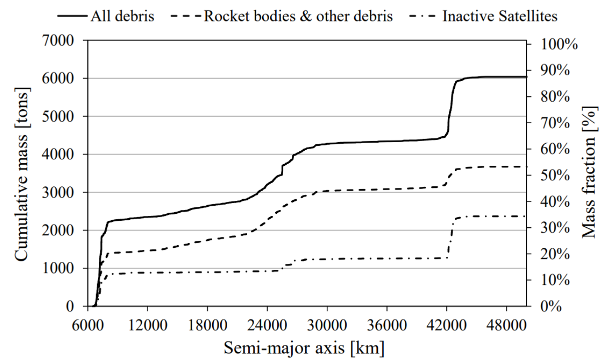

Figure 3. Cumulative mass distribution of the space debris dataset mapped onto debris semi-major axis.

Once again, two main areas of localized mass can be observed around LEO and GEO, located at semi-major axis values of <8378 km and 42164 km, respectively. Debris accumulation in LEO is limited through the 25-year rule mandated by the Inter-Agency Space Debris Coordination Committee (IADC) [11]. This is not the case for GEO, where despite its much lower launch cadence, more than 1600 tons of debris has accumulated over time. This sheer amount of mass highlights that the GEO graveyard orbit is an inherently unsustainable measure.

Beyond LEO and GEO, another region of clustered mass can be observed in Figure 3 between semi-major axis values of 22000 km and 30000 km. The majority of these debris objects are spent launch vehicle upper stages drifting in highly elliptical Geostationary Transfer Orbits (GTO) after delivering their payloads. The small number of inactive satellites in this orbital regime are primarily GPS and military satellites.

3.2 Resources & Reserves

The concept of resources and reserves is often used in geology when scoping out deposits of minerals or oil. The U.S. Geological Survey defines resources as "a concentration of naturally occurring solid, liquid, or gaseous material in or on the Earth's crust in such form and amount that economic extraction of a commodity from the concentration is currently or potentially feasible" [12]. Reserves are defined as "that part of an identified resource that meets specified minimum physical and chemical criteria related to current mining and production practices" [12]. This paper adapts this concept of resources and reserves in order to discern what part of the space debris dataset can be considered reserves for a recycling mission. The feasibility of recovery was used as the defining factor between resources and reserves. That is, resources were defined as the material currently in orbit or already on the Lunar surface, with reserves being the subset of these resources that are readily accessible and have potential for feasible recovery.

Figure 4 presents an overview of the space debris resources and reserves within the context of a European recycling mission for Lunar applications.

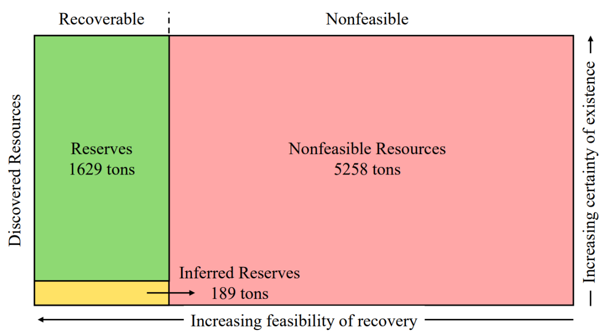

Figure 4. Overview of space debris resources and reserves.

The reserves consist primarily of European rocket bodies in higher orbits such as GTO (≈ 523 tons) and inactive, commercial satellites in the GEO graveyard orbit (≈ 1106 tons). The inferred reserves represent debris that is already on the Lunar surface. This includes crashed satellites, old rovers and landers. They are inferred because their exact state is unknown.

The remaining 74% of the space debris resources in the generated dataset were characterized as nonfeasible, which is a result of two main considerations. First, all non-European objects were omitted in accordance with the viewpoint of European autonomy established for this study. Military satellites were omitted for similar reasons. Commercially-operated objects were kept as they could potentially be bought after the end of their operational life. Second, all objects in LEO were omitted, as orbital transfer analyses indicated excessive propellant requirements compared to targets in higher energy orbits such as GTO or GEO. Finally, scientific satellites were omitted given that their unique designs would prevent the same debris recycling mission from being performed multiple times.

3.3 The Optimal Space Debris Target

Following the identification of space debris reserves, a trade-off process was used to determine the optimal space debris target for a recycling mission for Lunar applications. Within these reserves, it was found that spent Ariane upper stages in GTO are the optimal target for recovery and recycling. These high-mass objects have a high recoverable material mass content (up to 60% [13]) and their GTO orbits are prime staging points for an efficient transfer to the Moon. Finally, these stages present a substantial risk to operational space assets as they cross through the LEO protected zone at perigee and often also the GEO protected zone at their apogee. As such, removing these objects carries an inherent "value" beyond harvesting their raw materials. Table 1 shows the three most prominent Ariane upper stages drifting in GTO.

Table 1. Characteristics of the two most prevalent Ariane upper stages in GTO [6].

	Ariane 4 H10	Ariane 5 EPS	Ariane 5 ESC-A
Mass [kg]	1754 – 1920	1190 – 2850	5000
Orbit	GTO	GTO	GTO
$N_{objects}$	27	15	63
Materials	AA7020	AA7020	AA2219 & AA7020

Among these three targets, the Ariane 5 ESC-A upper stage was concluded to be the optimal space debris target due to its higher individual object mass and the larger number of objects currently in GTO. The latter is advantageous as it allows for the same recycling mission to be executed multiple times without major changes.

One of the key problems to be solved for debris mitigation missions as a whole is that high potential tumbling rates significantly complicate debris capture. The Kazan Federal University publishes a catalogue of tumbling rates based on optical observations from its MiniMegaTORTORA (MMT) system [14]. It was found through analysis of the 78 Ariane 5 rocket body objects that the rotation of effectively all of these stages is slowing down over time. Figure 5 highlights this increase in rotational period, which seems to follow an exponential growth as indicated by the dashed trendline.

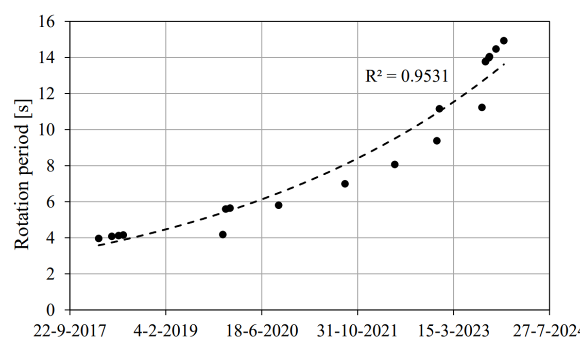

Figure 5. Tumbling behaviour over time for a selected ESC-A upper stage (NORAD 43176). Data from MMT catalogue [15] with added trendline.

Over time this observed breaking effect could widen the pool of objects that could be captured safely. The long orbital lifetimes of these stages in GTO substantiate this as a practical consideration.

4. Mission Design & Energy Analysis

With the ideal space debris target selected, the principle required input data and conditions are defined. This allows for the complete mission to be defined and analyzed within three distinct mission phases: launch, orbital transfer and debris processing.

4.1 Launch on Ariane 6

Following its recent maiden flight on the 9th of July 2024, Ariane 6 supersedes Ariane 5 as Europe's principle heavy-lift launch vehicle. Ariane 6 is capable of launching a high payload mass of 11500 kg directly into GTO [16], where the ESC-A space debris targets are located, all while maintaining the vision of European autonomy. This makes the utilization of Ariane 6 a natural choice for a space debris recycling mission concept. For this study, it was considered that all energy expended through the launch comes in principle from the combustion of the propellants. That is, the expended energy is equal to the available chemical energy within in the propellants which is liberated upon combustion. The stoichiometric reaction for the combustion of liquid hydrogen and liquid oxygen as used by Ariane 6 is:

$$2H_2(l) + O_2(l) \rightarrow 2H_2O(g) \tag{1}$$

Note that the Vulcain 2.1 and Vinci engines of Ariane 6 operate at non-stoichiometric Oxidizer to Fuel (O/F) ratios. This was accounted for by adapting the reaction for the excess fuel under the assumption of ideal combustion. The energy liberated from this reaction can be determined by calculating the change in enthalpy of the reaction, which is formulated in Equation 2 [17, 18].

$$\Delta_r H = \Sigma\left(n_{prod} H_{prod}\right) - \Sigma\left(n_{react} H_{react}\right) \tag{2}$$

Instead of assessing the total enthalpy, it is common to determine the standard enthalpy of reaction utilizing standard heats of formation as shown in Equation 3 [18]. The standard state here refers to 298.15 K.

$$\Delta_r H^\circ = \Sigma\left(n_{prod}\, \Delta_f H^\circ_{prod}\right) - \Sigma\left(n_{react}\, \Delta_f H^\circ_{react}\right) \tag{3}$$

Using this formulation is more practical for calculations as values for standard enthalpy of formation are extensively documented by various sources such as the National Institute of Standards and Technology (NIST) [19]. Adapting for the non-standard conditions of the cryogenic propellants used by Ariane 6 can then be done using Hess' law [16], which states the following:

$$\Delta_r H = \Delta_r H^\circ - \Delta H_{298K} \tag{4}$$

The same approach was used for the solid propellant P120 booster stages, accounting for the appropriate reaction equation for the HTPB 1912 propellants and the O/F ratio of the P120 engine. Converting the molar quantities to mass values of the distinct stages of Ariane 64, the following results were obtained.

Table 2. Energy expenditure analysis results for Ariane 6.

Stage	M_{prop} [kg]	E_{cost} [TJ]
Core stage	150000	1.797
Upper stage	30000	0.360
P120 Booster (4x)	4 x 143600	4 x 0.934
	Total	**5.893**

4.2 Orbital Transfers

A zero-patched conics approach was utilized for the orbital mechanics as a foundation to allow for the design and analysis of various orbital transfer strategies [20]. While Earth-Moon transfers are strong 3-body problems, the zero-patched conics approach was found to yield ΔV values within 1% to 6% accuracy depending on the transfer scenario, which was considered adequate for this preliminary study. The transfer vehicle dry mass was set at 1500 kg for the transfer analyses. This was based on the analysis of similar vehicles and extrapolating their payload mass to match the ESC-A. Two feasible transfer strategies were found: a direct, quasi-impulsive transfer using chemical propulsion, and a hybrid propulsion transfer using low-thrust propulsion.

4.2.1 Quasi-Impulsive Chemical Transfer

A standard, quasi-impulsive Hohmann transfer to the Moon was taken as the first baseline mission scenario to be analyzed. Though whereas the launch of traditional Moon missions can be targeted to facilitate favourable alignment for reaching the Moon, this is not the case for a space debris recycling mission. The capturing of debris prior to transfer imposes significant constraints on the transfer geometry, as the initial orbit is fixed by the specific targeted debris object. These upper stages in GTO have been subject to orbital perturbations for years, which have shifted their orbits continuously. This creates an alignment problem, highlighted in Figure 6, which shows the actual orbital orientation of two Ariane upper stages currently in orbit.

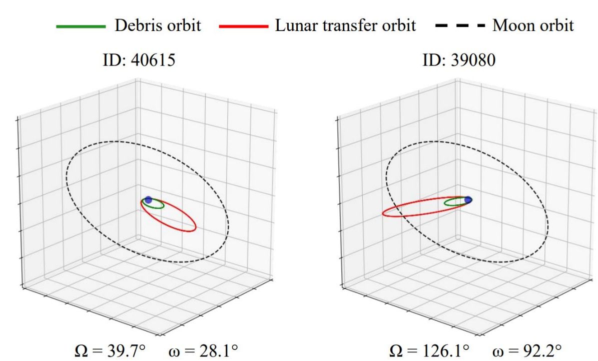

Figure 6. GTO orientation of actual Ariane upper stages.

Indeed, a standard transfer manoeuvre applied at perigee, shown in red, could miss the Moon entirely. The baseline assumption of an optimal aligned transfer geometry is therefore invalid for a space debris recycling mission. This orbital alignment problem was found to be one of the primary complications for a debris recycling mission targeting Lunar applications. The principle orbital perturbation in GTO was found to be the non-spherical shape of Earth's gravity field: the J_2 effect. The average secular rate of change in Argument of Periapsis (AoP) and Right Ascension of the Ascending Node (RAAN) can be determined using Equation 5 and 6 [21].

$$\dot{\omega} = \frac{3}{4} n J_2 \left(\frac{R_E}{p}\right)^2 (4 - 5 sin^2(i)) \quad (5)$$

$$\dot{\Omega} = -\frac{3}{2} n J_2 \left(\frac{R_E}{p}\right)^2 \cos(i) \quad (6)$$

This perturbing force can actually be used to create a favourable alignment by initiating a phasing period after debris capture in GTO. Propagation of the GTO orbit revealed that these rotations in AoP and RAAN create a combined motion in which the orbit path moves in a saddle-like shape, as shown in Figure 7.

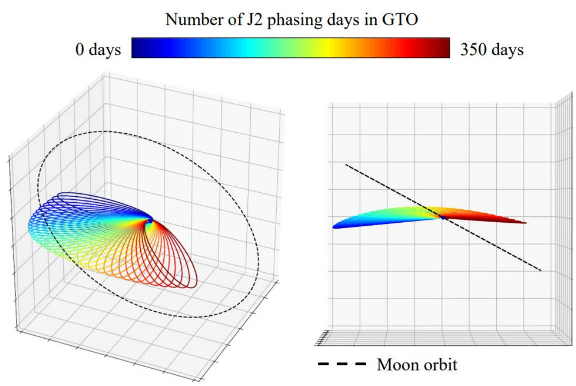

Figure 7. Lunar transfer orbit orientation after J2 phasing propagation in GTO, interval = 10 days.

It was found that, given any set position of the Moon, there are two unique combinations of RAAN and AoP for any particular debris orbit in GTO that lead to a suitable transfer alignment. The required phasing time depends on the initial conditions of the debris orbit, but is bound by a worst-case value of approximately 380 days to precess through half of a complete J_2 revolution. Additionally, since the line of apsides for this transfer may lie outside of the equatorial plane, the inclination difference between the transfer orbit and the Moon changes. This additional inclination change, in the worst case, is bound by a value equal to the GTO inclination.

Accounting for these worst-case situations, the transfer performance is summarized in Table 3. The energy cost for these manoeuvres was determined using the same method used for Ariane 6, though utilizing a Monomethyl Hydrazine (MMH) & Nitrogen Tetroxide (NTO) bi-propellant system. While toxic, MMH remains commonly used for Lunar missions, such as the European Service Module (ESM) and Chandrayaan 2 & 3.

Table 3. Orbital manoeuvre performance budgets for quasi-impulsive transfer mission scenario.

Manoeuvre	ΔV [km/s]	M_{prop} [kg]	E_{cost} [GJ]
Rendez-vous	0.182	498.3	3.2
TLI	0.747	2823.5	18.3
Lunar capture	0.919	2667.8	17.3
Descent injection	0.025	63.0	0.4
Landing termination	0.565	1281.1	8.3
Total	**2.437**	**7333.7**	**47.5**

Performing a soft landing was found to be infeasible due to excessive propellant mass requirements imposed by the large debris mass exceeding the launch capacity of Ariane 6. Instead, a final termination burn was applied to slow down the stack in a controlled crash onto the Lunar surface. A baseline value of 1200 m/s was used for the crash velocity, based on the range of 800 to 1600 m/s proposed by Koch [13], which facilitates debris break-up without vaporizing it. Through further it was found that this crash velocity could be reduced significantly without exceeding launch mass restrictions.

4.3 Low-Thrust Electric Hybrid Transfer

The implementation of low-thrust electric propulsion, with its substantially higher specific impulse, is an attractive way of reducing the propellant mass. Due to their low thrust levels, manoeuvre times are much longer in order to facilitate the total required impulse. This generally makes low-thrust propulsion unsuitable for manoeuvres that require high impulse over a short time, like Lunar capture. As such, a hybrid propulsion transfer was formulated based on the previous quasi-impulsive mission scenario though this time with the implementation of low-thrust propulsion for orbit-raising from GTO to Lunar intercept.

As low-thrust manoeuvres are substantially more complex to analyze than traditional impulsive manoeuvres, these were modelled using the FreeFlyer orbital simulation suite [22]. It was chosen to use 4 Busek BHT-6000 thrusters for the propulsion system, also used by the Lunar Gateway [23]. The simulated low-thrust trajectory from an initial GTO is presented in Figure 8.

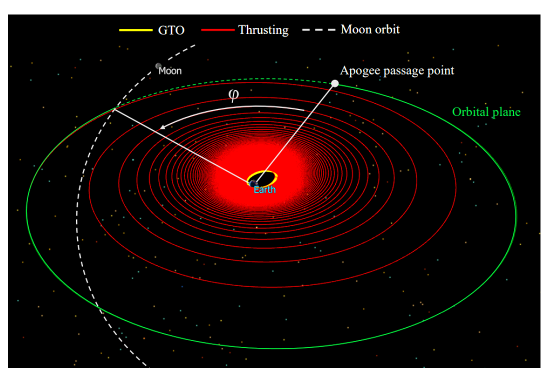

Figure 8. Simulated low-thrust trajectory from GTO to Lunar altitude at apogee, adapted to show alignment

However, Figure 8 shows that the alignment problem is also present for the low-thrust manoeuvre, as the apogee passage point is misaligned from the Moon's orbit by an angle φ. In order to solve this problem, a thrust-arcing approach was implemented in which thrust is only applied for true anomaly values θ < 180°. This effectively phases the apogee forward within in the orbital plane over time and allows for the manipulation of the orbit's orientation throughout the orbit-raising manoeuvre. Thrusting in the first half of the orbit compared to the second half is more efficient as it adds to the natural J_2 revolution early in the trajectory.

Figure 9 shows this method applied for the maximum required shift angle φ of 180° which ensures orbital transfer alignment can be achieved irrespective of the initial debris orbit orientation.

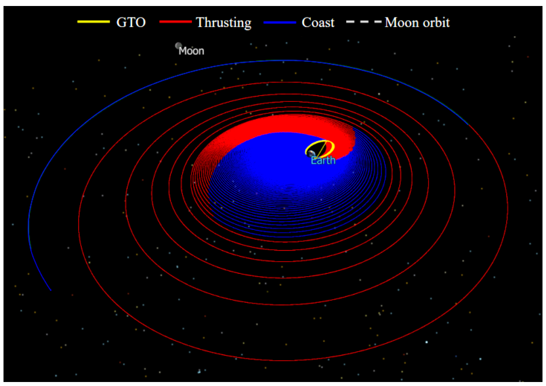

Figure 9. Simulated thrust-arcing trajectory from GTO to Lunar altitude at apogee, with 180° apogee shift.

This worst-case scenario yielded a total flight time of 636 days. While long flight times reduce the operational lifetime of conventional satellites, this is not a problem for a debris recycling mission. Since the transfer vehicle has no operational lifetime beyond the transfer phase, a long flight time is not an inherent problem. Using less engines reduces vehicle power requirements without changing ΔV, though at the cost of longer flight time.

Following optimization of the simulation for minimum propellant usage and adapting the outputs into the defined zero-patched conics approach, the transfer performance results for this mission scenario is shown in Table 4. Note that the energy cost of the low-thrust orbit raising manoeuvre is by definition equal to zero as the solar electric power used to operate the electric propulsion is obtained effectively for free from the Sun.

Table 4. Orbital manoeuvre performance budgets for low-thrust hybrid transfer mission scenario.

Manoeuvre	**ΔV [km/s]**	**M_{prop} [kg]**	**E_{cost} [GJ]**
Rendez-vous	0.182	393.2	2.5
Low-thrust orbit raising	3.368	1379.0	0
Lunar capture	0.823	2354.3	15.3
Descent injection	0.025	63.0	0.4
Landing termination	0.565	1281.1	8.3
Total	**2.437**	**5469.6**	**26.5**

4.4 Debris Processing on the Lunar Surface

For this study, it was assumed that following the controlled crash onto the Lunar surface, space debris scrap of moderate size could be collected in a way that is suitable for rover transportation to the recycling site for further processing and final utilization at least in a semi-autonomous fashion. Re-melting the debris is an important step to reshape the material, drawing heavily upon well-understood terrestrial recycling processes for metals. As such, simple thermal re-melting processes were considered ideal. Inductive heating was concluded to be the most suitable re-melting technique. Such inductive heating furnaces use only electrical energy and are widely used in the terrestrial recycling industry while also being readily adaptable to the vacuum conditions of the Moon.

To assess the energy required for the inductive heating of the salvaged debris, Equation 7 was set up. This heat equation details the determination of the total theoretical energy required for heating and melting a material mass M from an initial temperature T_0 to a final pouring temperature T_{pour}.

$$Q = M\left[C_{p_{solid}}(T_{melt} - T_0) + L_{fusion} + C_{p_{liquid}}(T_{pour} - T_{melt})\right] \quad (7)$$

The specific heat is not constant, but rather it varies with temperature and phase, which was estimated using the Shomate equation shown in Equation 8 [19].

$$C_p = A + Bt + Ct^2 + Dt^3 + \frac{E}{t^2} \quad (8)$$

Where t is the temperature in Kelvin divided by 1000. The variables A, B, C, D and E in this formulation are experimentally determined constants obtained from the NIST [19]. Using an initial Lunar surface temperature of 48.5 °C based on measurements by Chandrayaan-3 [24] and a furnace efficiency of 90%, a heat value of 1.548 MJ/kg of aluminium was found.

Finally, the casting of molten aluminium into feedstock material was chosen as the utilization to complete the creation of new raw materials. A value of 0.211 kWh (0.760 MJ) per kg of aluminium was taken from terrestrial primary recycling industry. As such, a total output energy of 2.31 MJ/kg is required for the complete recycling process. Accounting for an assumed electrical circuit efficiency of 25%, including solar cell efficiency, a total solar energy usage of 9.23 MJ/kg of aluminium. Given a dry mass of 5000 kg for the ESC-A target and a 60% raw material fraction, a total energy of 27.7 GJ is required for the recycling of a complete ESC-A upper stage.

4.5 Alternative Argonaut Mission Scenario

While a direct raw material delivery mission to the Lunar surface does not have to rely on any in-situ recycling operations, the energy cost associated with the manufacturing of the delivered raw materials must not be omitted. The overall process cycle for this primary production is well understood and documented. Choate and Green [5] report a total required onsite energy of 89.42 MJ/kg for the primary production aluminium. Note however that a distinction was made between onsite energy usage (i.e. the energy used within the production facilities) and ”tacit” energy. This tacit or gross energy includes secondary energy required for producing electric energy and raw materials expended in the production. Accounting for sustainable energy generation, the US grid for the aluminium industry consumes on average 3.01 kWh of chemical (fuel) energy to supply 1 kWh of electrical energy [5]. With this in mind, the total tacit energy cost of primary aluminium production is equal to 224.14 MJ/kg. Therefore, a total energy of 470.70 GJ is required to manufacture the Argonaut's maximum 2100 kg payload.

For the orbital transfer, the Argonaut is put directly onto a Lunar Transfer Orbit (LTO) by Ariane 64. As the Argonaut uses a chemical bipropellant (MMH & MON3) system [25], a quasi-impulsive manoeuvre method was used again to analyze the orbital transfer. Adopting the input conditions of the LTO and accounting for a soft landing, the transfer performance is shown in Table 5.

Table 5. Orbital manoeuvre performance budgets for Argonaut mission scenario.

Manoeuvre	ΔV [km/s]	M_{prop} [kg]	E_{cost} [GJ]
Lunar capture	0.910	2288.0	14.8
Descent injection	0.025	54.6	0.4
Landing termination	1.885	3045.4	19.7
Total	**2.820**	**5388.0**	**34.9**

5. Results

Compiling the outputs obtained throughout the analyses, a combined, global mission energy analysis was performed. This analysis formed the basis for the comparative analysis between the defined mission scenarios and the alternative mission scenario utilizing the Argonaut lander.

5.1 Specific Global Mission Energy Cost

Rather than comparing a total embodied energy cost, a specific energy cost, i.e. the energy cost per kg of raw material delivered was defined. This represents the energy investment corrected for an analogous raw material to create an equivalent comparative analysis across the various mission scenarios. Figure 10 presents the results of the specific global mission energy analysis. The distinction between total energy use and energy cost is important again here, as solar energy by definition does not represent an actual energy investment and therefore does not contribute to energy cost. This is in contrast to other energy expenditures such as the combustion of propellants, which constitute to a strict energy loss.

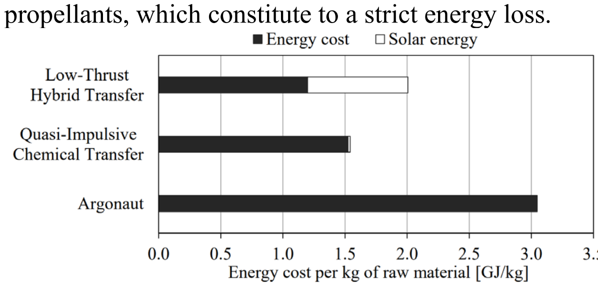

Figure 10. Specific global mission energy cost comparison.

Both recycling mission concepts result in a 31% lower specific energy cost than a conventional material delivery mission. This is primarily due to their substantially larger returned material mass. Capturing payload mass in orbit circumvents the strict launch mass constraints which limit the payload mass for traditional landers. It was found that launch dominates the energy analysis, with energy costs one or even two orders of magnitude larger than the other processes. For a space debris recycling mission, this excessive launch energy associated with the payload material has already been provided by the original mission that left this material in orbit in the first place.

5.2 Launch Optimization Through Rideshare

Capturing payload mass in orbit significantly reduces the required vehicle launch mass. Whereas the Argonaut requires a dedicated launch of Ariane 64 to put it directly on its LTO, this is not the case for the space debris recycling missions. The transfer vehicle wet masses of 8834 kg and 6970 kg for the quasi-impulsive and low-thrust hybrid transfer mission scenarios, leave substantial margin within the 11500 kg payload mass capacity of Ariane 64 to GTO. This margin could be utilized by introducing a secondary client in a rideshare configuration through Ariane's dual payload integration.

This reduces the global mission energy cost by reducing the launch energy proportionally to the launch vehicle payload mass capacity utilization. The targeting of ESC-A upper stage debris objects in GTO makes GEO missions the primary candidates for inclusion as rideshare clients. The historical launch mass for GEO satellites, obtained from the Union of Concerned Scientists [26], in Figure 11 indicates that numerous clients exist that fit in the leftover payload mass margin.

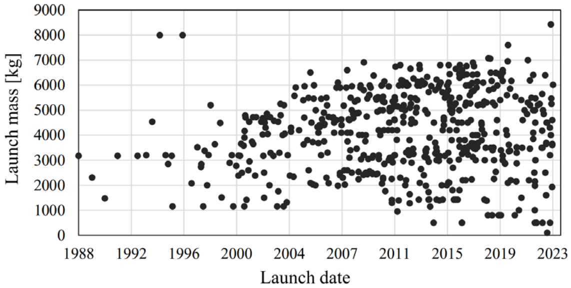

Figure 11. Launch mass distribution of GEO satellites.

The only constraint for a rideshare configuration is that a target must be chosen that naturally approaches an AoP value of 0° or 180° to facilitate client insertion into GEO. The wide spread of AoP values within the ESC-A population combined with the natural J_2 motion makes choosing a target based on this constraint a viable option. This proportional launch vehicle utilization was also applied by Wilson and Vasile [27] when studying the environmental impacts of space missions. Accounting for this launch optimization through rideshare, the updated specific global mission energy analysis results are presented in Figure 12.

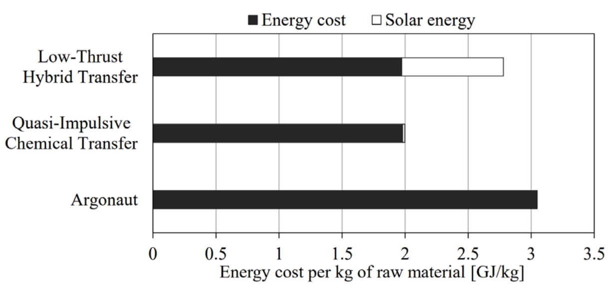

Figure 12. Specific global mission energy cost comparison adapted for launch vehicle payload capacity utilization.

A total specific energy cost reduction of 50% and 61% is observed for the quasi-impulsive and low-thrust hybrid transfer mission scenarios, respectively compared to the conventional lander mission. This substantial reduction reaffirms the importance of the launch as the dominant energy sink and the benefit of reducing launch mass by capturing debris in orbit rather as payload. Wilson and Vasile [27] concluded that the launch also dominates the environmental impacts and carbon footprint of space missions. As such, the more efficient use of the launch vehicle also significantly reduces the environmental impacts and carbon footprint of debris recycling missions.

When comparing the two debris recycling mission concepts directly however, practical aspects of a mission can justify an increased energy expenditure. The implementation of electric propulsion, despite resulting in lower specific energy cost, increases mission complexity. The long low-thrust spiral trajectory is more susceptible to Luni-Solar interactions, which complicates mission planning. Additionally, high power requirements and long flight times drive up vehicle complexity and cost. A conventional, direct Lunar transfer using chemical propulsion is significantly simpler and faster. For novel, complex missions, simplifying the process chain can be ideal whenever possible and practical. As such, sacrificing the additional 11% energy cost reduction could potentially be justified.

5.3 Sensitivity Analysis

The work presented in this paper relies on several mission-critical assumptions. A sensitivity analysis was conducted to study the impact of variations in these assumptions on the results. The raw material mass fraction of upper stages is the principal assumption, as it directly influences the mass that can be recovered. Figure 13 presents the impact of raw material mass fractions lowered from the baseline of 60%.

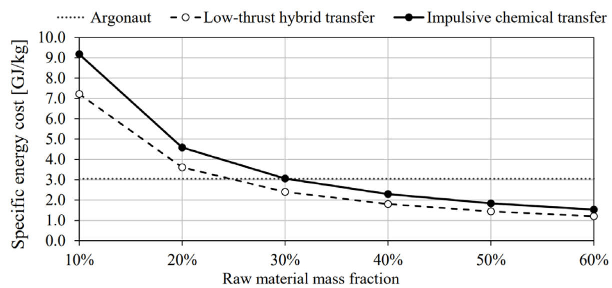

Figure 13. Specific energy cost as function of assumed raw material mass fraction.

The intersections with the dotted line represent the break-even points, which are 30% and 24% for the quasi-impulsive and low-thrust hybrid transfer mission scenarios, respectively. As such, significant margin exists for lower raw material mass fractions while maintaining a lower specific energy cost. The crash velocity of the transfer vehicle and the debris object is the second main assumption. Figure 14 presents the impact of lowering the crash velocity on the specific energy cost.

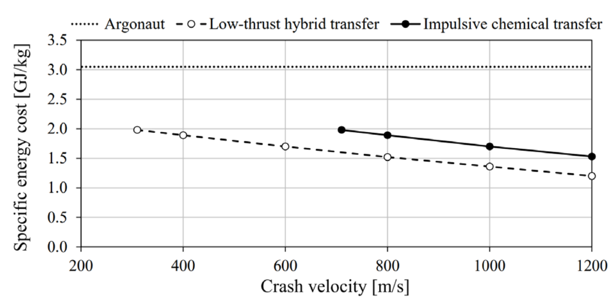

Figure 14. Specific energy cost as function of assumed debris crash velocity onto the Lunar surface.

Here too, significant margin exists to lower the crash velocity while maintaining a lower specific energy cost. The reduction in impact velocity is limited by launch vehicle payload capacity, as more propellant is required for all manoeuvres. This limit was reached at 710 m/s and 310 m/s for the quasi-impulsive and low-thrust hybrid transfer mission scenarios, respectively.

6. Conclusions & Next Steps

This paper has shown that strong potential exists for a space debris recycling mission to be both feasible and viable as a means of supplying raw material resources to the Lunar surface with substantial reductions in energy cost per kg compared to a conventional lander mission. By capturing their principal payload mass in orbit, debris recycling missions save significant payload mass margin of the Ariane 64 launch vehicle, which is what ultimately defines their viability compared to traditional Lunar lander missions like the Argonaut. Beyond the potential for greater energy efficiency, the ”value” of removing debris cannot be understated. Removing high-risk objects such as upper stages in GTO is a key step on the road towards a zero debris environment, as no long-term mitigation strategies for such objects currently exist. The recycling of space debris allows for the creation of value which traditional space debris mitigation missions have critically lacked. The work performed forms a fundamental baseline of understanding through the assessment of feasibility and viability as cornerstones. The margin of efficiency that can potentially be gained as shown in this study indicates that the concept of space debris recycling warrants further study. Additionally, the notion of resources and reserves was adapted from terrestrial geology to characterize the space debris dataset. This new perspective has potential to benefit the entire field of space debris recycling.

Efforts towards a debris recycling mission could already be started today. A precursor CubeSat mission could be used to rendez-vous with an ESC-A in GTO to validate its tumbling behaviour with optical observations. Subsequent larger missions could attempt capture of such upper stages similar to Astroscale’s mission to capture one of the JAXA H-2A upper stages [28]. Additionally, the characteristics of hyper-velocity debris impacts on the Moon could be studied by using Moon-orbiting satellites to make observations of known crash sites of rocket stages on the Lunar surface. The Lunar Reconnaissance Orbiter and Chandrayaan-2 are prime candidates for such observations.

Acknowledgements

Y. Heumassej would like to thank ESA and TU Delft for their continued support and the opportunity to conduct the study detailed in this paper.

References

[1] European Space Agency, ESA’s Annual Space Environment Report, 19 July 2024.
[2] European Space Agency, Argonaut, 2023 https://www.esa.int/Science_Exploration/Human_and_Robotic_Exploration/Exploration/Argonaut (accessed 08/11/2023).
[3] Davies, P., Ariane 6 launch: Why it matters for Europe's space ambitions, Euronews, 7 July 2024 https://www.euronews.com/next/2024/07/09/ariane-6-launch-how-to-watch-it-and-why-it-matters-for-europes-space-ambitions (accessed 23/08/2024).
[4] Hill, E., Mellin, M. J., Deane, B., Liu, Y., and Taylor, L. A., Apollo sample 70051 and high- and low-Ti lunar soil simulants MLS-1A and JSC-1A: Implications for future lunar exploration, Journal of Geophysical Research 112, 2 February 2007, DOI: 10.1029/2006JE002767.
[5] Choate, W. T. and Green, J. S. U.S. Energy Requirements for Aluminum Production Historical Perspective, Theoretical Limits and Current Practices. Business Consulting and Services (BCS) LLC, U.S. Department of Energy: Industrial Technologies Program, February 2007.
[6] Gallbrecht, M. M., Cervone, A., Vincent-Bonnieu, S., The Moon as an effective propellant source: A comprehensive exergy analysis from extraction to depot, Acta Astronautica 218, 24 February 2024, DOI: 10.1016/j.actaastro.2024.02.035
[7] European Space Agency, DISCOSweb, https://discosweb.esoc.esa.int/ (accessed 16/05/2023).
[8] Kelso, T. S., CelesTrak, 2023, https://celestrak.org/ (accessed on 28/05/2023).
[9] United States Space Command, Space-Track, 2023, https://www.space-track.org/ (accessed 31/05/2023).
[10] Anderson, P. V., McKnight, D. S., Di Pentino, F., Schaub, H., Operational Considerations of GEO Debris Synchronization Dynamics, Proceedings of the 66th International Astronautical Congress, 2015
[11] Inter-Agency Space Debris Coordination Committee (IADC), IADC Space Debris Mitigation Guidelines: Revision 3, 23 June 2021.
[12] United States Geological Survey, Principles of a Resource/Reserve classification for minerals: Geological Survey Circular 831, 1980.
[13] Koch, F., A Business Case for Space Debris: Analysis of space debris recycling potential to supply raw materials for construction on the Moon, Orbit Recycling, European Space Agency, July 2021.
[14] Biryukov, A., Beskin, G., Karpov, S., Bondar, S., Ivanov, E., Katkova, E., Perkov, A., and Sasyuk, V., The first light of Mini-MegaTORTORA wide-field monitoring system, Baltic Astronomy 24, 6 January 2015, DOI: 10.1515/astro-2017-0208.

[15] Katkova, E., Satellites identified in MMT data, Kazan Federal University, 5 August 2024, http://mmt9.ru/satellites/ (accessed on 16/02/2024).
[16] ArianeSpace, Ariane 6 User's Manual, Version 2, Revision 0, February 2021.
[17] Zandbergen, B. T. C., AE4-S01: Thermal Rocket Propulsion: Version 2.08, Delft University of Technology, August 2020.
[18] Sutton, G. P. and Biblarz, O., Rocket Propulsion Elements, 9th ed, Hoboken, New Jersey: John Wiley & Sons, 2001.
[19] Linstrom, P. J. and Mallard, W. G., NIST Chemistry WebBook: NIST Standard Reference Database Number 69. National Institute of Standards and Technology, 2023, DOI: https://doi.org/ 10.18434/T4D303.
[20] Uphoff, C., Practical Aspects of Transfer from GTO to Lunar Orbit, Flight Mechanics: Estimation Theory Symposium 1993, Ball Corporation, February 1993.
[21] Wertz, J. R., Orbit & Constellation Design & Management, Microcosm Press, Hawthorne, California, 2001.
[22] A.I. Solutions, FreeFlyer Astrodynamics Software, 2024 https://ai-solutions.com/freeflyer-astrodynamic-software/ (accessed 21/11/2023)
[23] Herman, D. A., Gray, T., Johnson, I., Kerl, T., Lee, T., and Silva, T., The Application of Advanced Electric Propulsion on the NASA Power and Propulsion Element (PPE), 36th International Electric Propulsion Conference, Vienna, Austria. University of Vienna, September 2019.
[24] Indian Space Research Organisation (ISRO), Chandrayaan-3 Mission, August 2023, https://twitter.com/isro/status/1695725102166671448? (accessed 24/11/2023).
[25] Liggieri, G., Boiron, A., Hansen, B. E., Josefsen, H., Worsley, E., Haynes, A., and Shaw, M., RELIANCE Design, Manufacturing and Testing of the Breadboard Engine, Aerospace Europe Conference 2023 - 10th EUCASS - 9th CEAS, July 2023, DOI: 10.13009/EUCASS2023-470.
[26] Grimwood, T., UCS Satellite Database, Union of Concerned Scientists (UCS), May 2023, http://www.ucsusa.org/satellite_database (accessed 18/12/2023)
[27] Wilson, A. R., Vasile, M., Life cycle engineering of space systems: Preliminary findings, Advances in Space Research 72, 18 January 2023, DOI: 10.1016/j.asr.2023.01.023
[28] Japan Aerospace Exploration Agency (JAXA), CRD2: Commercial removal of Debris Demonstration, 2024 https://www.kenkai.jaxa.jp/eng/crd2/ (accessed 26/08/2024).